JACS
JOURNAL OF THE AMERICAN CHEMICAL SOCIETY
Article
pubs.acs.org/JACS

Versatile Reactivity of a Four-Coordinate Scandium Phosphinidene Complex: Reduction, Addition, and CO Activation Reactions

Yingdong Lv,[†] Christos E. Kefalidis,[‡] Jiliang Zhou,[†] Laurent Maron,*[,‡] Xuebing Leng,[†] and Yaofeng Chen*[,†]

[†]State Key Laboratory of Organometallic Chemistry, Shanghai Institute of Organic Chemistry, Chinese Academy of Sciences, 345 Lingling Road, Shanghai 200032, People's Republic of China

[‡]LPCNO, CNRS, and INSA, Université Paul Sabatier, 135 Avenue de Rangueil, Toulouse 31077, France

Supporting Information

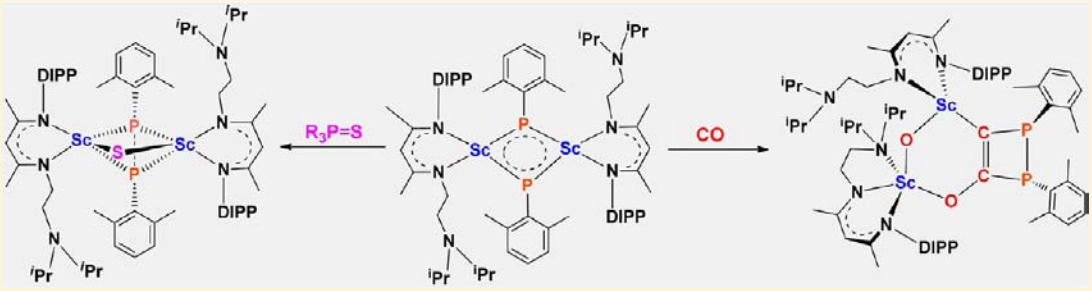

ABSTRACT: The four-coordinate scandium phosphinidene complex, $[LSc(\mu\text{-PAr})]_2$ (L = (MeC(NDIPP)CHC(Me)-($NCH_2CH_2N(^iPr)_2$)), DIPP = 2,6-$(^iPr)_2C_6H_3$; Ar = 2,6-$Me_2C_6H_3$) (**1**), has been synthesized in good yield, and its reactivity has been investigated. Although **1** has a bis(μ-phosphinidene)discandium structural unit, this coordinatively unsaturated complex shows high and versatile reactivity toward a variety of substrates. First, two-electron reduction occurs when substrates as 2,2′-bipyridine, elemental selenium, elemental tellurium, $Me_3P{=}S$, or $Ph_3P{=}E$ (E = S, Se) is used, resulting in the oxidative coupling of two phosphinidene ligands $2[PAr]^{2-}$ into a diphosphene ligand $[ArP\text{-}PAr]^{2-}$. Complex **1** easily undergoes nucleophilic addition reactions with unsaturated substrates, such as benzylallene, benzonitrile, *tert*-butyl isocyanide, and CS_2. This complex also shows a peculiar reactivity to CO and $Mo(CO)_6$, that includes C−P bond formation, C−C coupling and C−O bond cleavage of CO, to afford novel phosphorus-containing products. In the last two types of reactivity, reaction profiles have been computed (for the insertion of ^{t}BuNC and the CO activation by **1**) at the DFT level. The unexpected/surprising sequence of steps in the latter case is also revealed.

1. INTRODUCTION

As the phosphorus analogues of alkylidene (or carbene) and imido (or nitrene) complexes, phosphinidene complexes have received much attention.[1] Their studies revealed that the terminal phosphinidene monometallic complexes, both nucleophilic and electrophilic types, (coordination types **A** and **B** in Chart 1), are highly reactive, resulting in new phosphorus-containing molecules, but also more efficient phosphorus−element bond synthesis and useful catalytic transformations.[1] Recently, Ruiz and co-workers showed that bimetallic iron complexes $[Fe_2(\eta^5\text{-}C_5H_5)_2(\mu\text{-PR})(\mu\text{-CO})(CO)_2]$ containing bent phosphinidene bridges (type **C**) display interesting reactivity. Indeed, the lone pair of the phosphorus atom of this species leads to reactivity toward electrophiles such as alkyl halides, chalcogens, organic azides, diazoalkanes, ethanol, alkenes, alkynes, and metal carbonyls.[2] Some representative reactions are shown in Scheme 1. Ruiz and co-workers also uncovered that the bimetallic molybdenum phosphinidene complex $[Mo_2Cp(\mu\text{-}\kappa^1{:}\kappa^1,\eta^5\text{-}PC_5H_4)(\eta^6\text{-}1,3,5\text{-}C_6H_3{}^tBu_3)(CO)_2]$ (type **D**) undergoes addition reactions with activated alkenes or alkynes[3a−c] and metal carbonyls.[3a,d] Contrariwise, bridged phosphinidene complexes of type **E** are sluggish, and

Chart 1

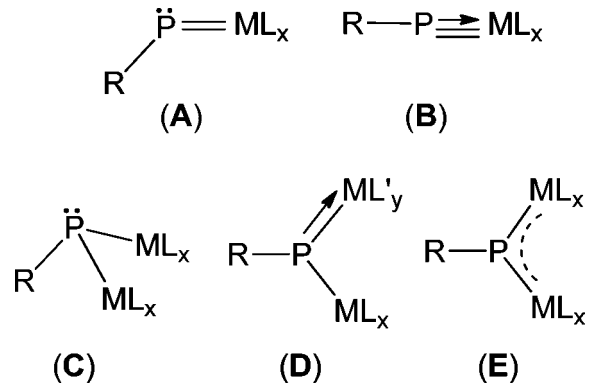

Received: June 27, 2013
Published: September 4, 2013

dx.doi.org/10.1021/ja406413d | J. Am. Chem. Soc. 2013, 135, 14784−14796

Scheme 1. Representative Reactions of $[Fe_2(\eta^5\text{-}C_5H_5)_2(\mu\text{-}PR)(\mu\text{-}CO)(CO)_2]$

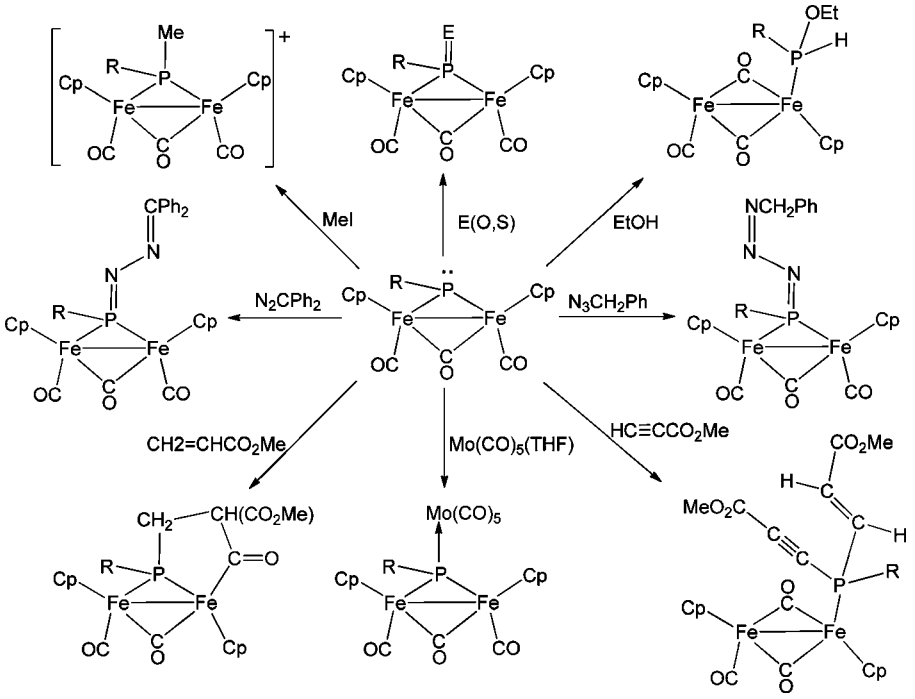

Scheme 2. Synthesis of Sc Phosphinidene Complex 1 and Its Reactivity With 4-Dimethylamino Pyridine

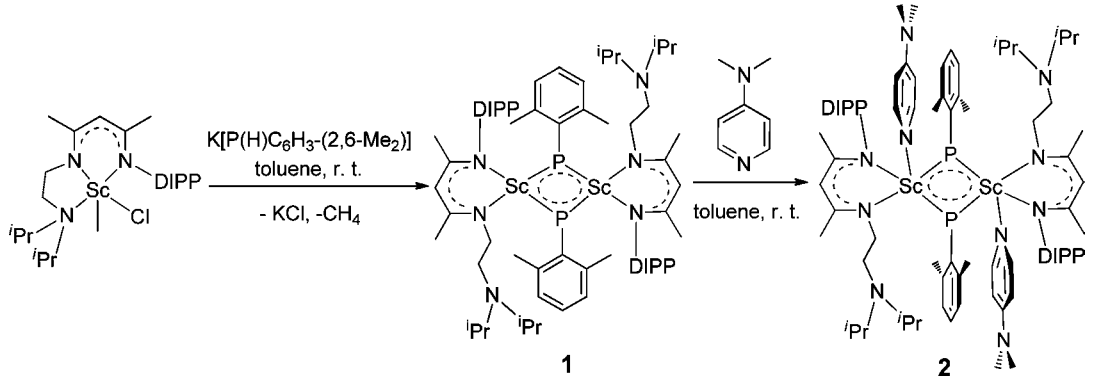

their reactivity is mainly attributed to the nucleophilicity and reducibility of the phosphorus atoms.[4] For example, coordination of Lewis bases has been reported giving acid−base adducts as well as oxidation reactions with organic azides, diazoalkanes, or S_8 yielding oxidation products containing P═X (X = NR, CR_2, or S) fragments. Ruiz and co-workers also found that the Mo−P bond of $[Mo_2Cp_2(\mu\text{-}PR)(CO)_4]$ (type **E**) becomes active only at high temperature (ca. 438 K) or under exposure to near UV−vis or UV light.[5]

Since rare-earth metal (Sc, Y, and lanthanide metal) ions are among the hardest Lewis acids and phosphinidene ligands are soft Lewis bases, rare-earth metal−phosphinidene coordination is thus mismatched based on the Pearson's HSAB principle.[6] Rare-earth metal complexes containing phosphinidene bridges could not be synthesized until recently,[7] and the synthesis of the terminal species has not been achieved so far. Thus, the reactivity of such complexes remains largely unexplored. Kiplinger's group and our group showed that these complexes can deliver the phosphinidene unit to ketones,[7a,b] and Mindiola and co-workers found that the five-coordinate scandium bridged phosphinidene complex supported by PNP ligand is sluggish, but the Sc−Li phosphinidene ate complex can deliver the phosphinidene unit not only to ketones but also to phosphorus dichlorides and metal chorides.[7c] Recently, we developed and synthesized a type of β-diketiminato-based tridentate ligands[8] as well as structurally characterized a Sc terminal imido complex by employing one of these ligands.[9] In attempts to synthesize the Sc terminal phosphinidene complexes by using these tridentate ligands, we obtained a four-coordinate bis-scandium bridged phosphinidene complex of coordination type **E**. Interestingly, this complex shows high and intriguing reactivity under mild conditions, which is distinct from those already reported for other transition-metal bridged phosphinidene complexes. For instance, it reduces 2,2′-bipyridine, phosphine sulfide, phosphine selenide, elemental selenium, and elemental tellurium. It also undergoes nucleophilic addition with unsaturated substrates, such as allene, nitrile, isocyanide, and CS_2. Most fascinatingly, this complex reacts with CO to afford a novel phosphorus-containing product, exhibiting a four-membered C_2P_2 ring. The latter is achieved through a sequence of C−P bond

dx.doi.org/10.1021/ja406413d | J. Am. Chem. Soc. 2013, 135, 14784−14796

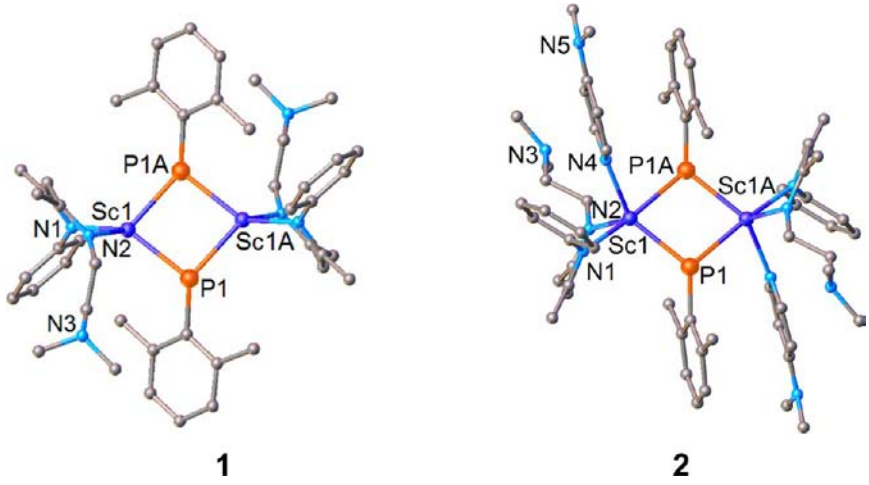

Figure 1. Molecular structures of **1** and **2**. Isopropyl groups of the amino arm are represented by only one carbon atom; isopropyl groups on the arene and all H-atoms are omitted for clarity. Selected metrical parameters (distances in angstroms; angles in degrees) for **1**: Sc1−N1 = 2.115(3), Sc1−N2 = 2.126(3), Sc1−P1 = 2.522(1), Sc1−P1A = 2.528(1); Sc1−P1−Sc1A = 92.79(3), P1−Sc1−P1A = 87.21(3). For **2**: Sc1−N1 = 2.212(3), Sc−N2 = 2.141(3), Sc−N4 = 2.351(3), Sc1−P1 = 2.540(1), Sc1−P1A = 2.589(1); Sc1−P1−Sc1A = 99.03(4), P1−Sc1−P1A = 80.98(4).

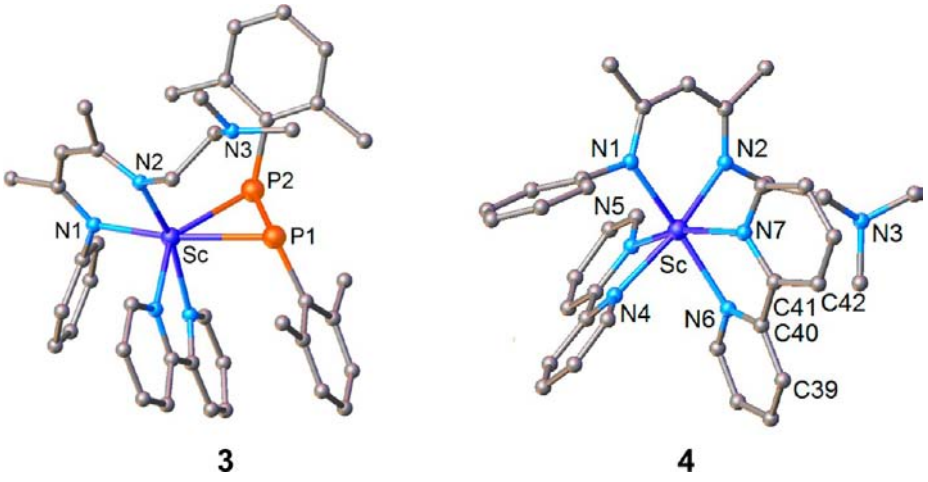

Figure 2. Molecular structures of complexes **3** and **4**. Isopropyl groups of the amino arm are represented by only one carbon atom; isopropyl groups on the arene and all H-atoms are omitted for clarity. Selected metrical parameters (distances in angstroms; angles in degrees) for **3**: Sc−N1 = 2.223(5), Sc−N2 = 2.185(5), Sc−P1 = 2.661(2), Sc−P2 = 2.611(2), P1−P2 = 2.194(2); P2−Sc−P1 = 49.17(5), P2−P1−Sc = 64.22(6), P1−P2−Sc = 66.61(6). For **4**: Sc−N1 = 2.231(2), Sc−N2 = 2.176(3), Sc−N4 = 2.218(3), Sc−N5 = 2.235(2), Sc−N6 = 2.249(2), Sc−N7 = 2.197(2), C39−C40 = 1.410(4), C40−C41 = 1.421(4), C41−C42 = 1.421(4); N2−Sc−N4 = 162.95(9), N1−Sc−N6 = 159.97(9), N5−Sc−N7 = 160.54(9), N5−Sc−N4 = 72.41(9), N6−Sc−N7 = 71.70(9).

formation, C−C coupling, C−O bond cleavage, and P−P coupling, as it is revealed by computational mechanistic studies.

2. RESULTS AND DISCUSSION

Synthesis and Crystal Structure of the Four-Coordinate Scandium Phosphinidene Complex (1). Reaction of Sc methyl chloride complex [LSc(Me)Cl] (L = (MeC(NDIPP)CHC(Me)(NCH$_2$CH$_2$N(^{i}Pr)$_2$)), DIPP = 2,6-(^{i}Pr)$_2$C$_6$H$_3$) with 1 equiv of K[P(H)C$_6$H$_3$-(2,6-Me$_2$)] in toluene at room temperature yielded a Sc bridged phosphinidene complex [LSc(μ-PAr)]$_2$ (Ar = 2,6-Me$_2$C$_6$H$_3$) (**1**) in 74% yield (Scheme 2). The NMR spectral monitoring of the reaction in C$_6$D$_6$ showed that a transient phosphido−methyl complex was formed initially, which converted into **1** via methane elimination at room temperature. Complex **1** was characterized by NMR spectroscopy, elemental analysis, and single crystal X-ray diffraction. The latter revealed there are two crystallographically independent molecules in the unit cell of **1**, and both of them are centrosymmetric with the phosphinidene ligand [PAr]$^{2-}$ coordinated to two Sc centers with two nearly equivalent Sc−P bonds (2.522(1) and 2.528(1) Å, or 2.517(1) and 2.524(1) Å) (Figure 1). In addition, the amino side arm of the tridentate nitrogen ligand (L) is not coordinated to the Sc center. In line with what observed in the solid state, the ^{1}H NMR spectrum of complex **1** in C$_6$D$_6$ displays two triplets at δ = 4.44 and 2.70 ppm, respectively. These peaks are attributed to the four hydrogen atoms of the −NCH$_2$CH$_2$N− fragment of the tridentate nitrogen ligand, revealing that the two hydrogen atoms of each CH$_2$ unit of −NCH$_2$CH$_2$N− are equivalent. This is different from that of the Sc methyl chloride complex [LSc(Me)Cl], which displays four signals for those four hydrogen atoms. Therefore, in complex **1** the metal centers are four-coordinate, being less coordinatively saturated than the reported rare-earth metal bridged phosphinidene complexes. For example, the Lu and Sc bridged phosphinidene complexes supported by PNP ligands [(PNP)Ln(μ-PAr)]$_2$ (Ln = Lu or Sc;

dx.doi.org/10.1021/ja406413d | J. Am. Chem. Soc. 2013, 135, 14784−14796

Scheme 3. Reaction of Complex 1 with 2,2′-Bipyridine

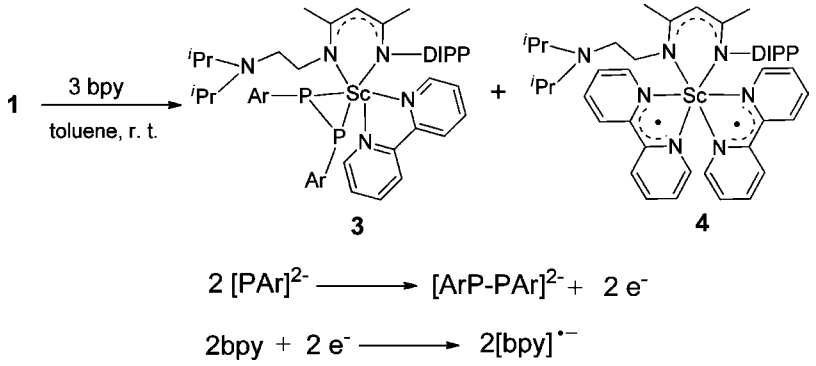

Ar = 2,4,6-Me_3-C_6H_2 or 2,4,6-$^i Pr_3C_6H_2$) have five-coordinate metal centers.[7a,c] Finally, the ^{31}P NMR spectrum of **1** displays a singlet at δ = 183.8 ppm, in line with a symmetrical coordination of each phosphorus.

In attempts to synthesize a Sc terminal phosphinidene complex, addition of a strong donor 4-dimethylamino pyridine (DMAP) to **1** was carried out. Reaction of **1** with 2 equiv of DMAP in toluene gave a DMAP coordinated Sc phosphinidene complex $[LSc(DMAP)(\mu\text{-PAr})]_2$ (Ar = 2,6-$Me_2C_6H_3$) (**2**) in 90% yield. Complex **2** is a centrosymmetric dimer and retains the bis(μ-phosphinidene)discandium structural unit (Figure 1). The Sc−P bonds (2.540 (1) and 2.589 (1) Å) are slightly longer than those in **1** (2.517(1) and 2.528(1) Å). The dihedral angle between the 2,6-dimethylphenyl ring and the Sc_2P_2 plane (89.5°) is significantly larger than in **1** (36.2° or 39.1°), which minimizes DMAP−phosphinidene repulsions. Reaction of **1** with 4 equiv of DMAP was also investigated, which gave complex **2** and 2 equiv of unreacted DMAP.

Reductive Chemistry of the Scandium Phosphinidene Complex. As DMAP is unable to break the bis(μ-phosphinidene) unit, the addition of a bidentate ligand 2,2′-bipyridine (bpy) to **1** was subsequently investigated. The reaction was monitored by NMR spectroscopy in C_6D_6 at room temperature. The ^{31}P NMR spectrum showed the formation of a new complex, which displays two doublets at δ = 30.0 and 25.9 ppm, as well as some remaining complex **1**, when 1 or 2 equiv of bpy were used. When the amount of bpy was increased up to 3 equiv, complex **1** was completely consumed. The reaction of **1** with 3 equiv of bpy was subsequently scaled up in toluene, which gave complexes **3** and **4**. The molecular structures of **3** and **4** are shown in Figure 2. Complex **3** is a Sc diphosphene complex [LSc(bpy)(ArP-PAr)], while complex **4** contains two bpy radical-anions, $[LSc(bpy)_2]$, as shown in Scheme 3. Therefore, in the reaction of **1** with bpy, two dianionic phosphinidene ligands $2[PAr]^{2-}$ are oxidatively coupled to form a dianionic diphosphene ligand $[ArP\text{-}PAr]^{2-}$ in **3** and reduce two bpy to afford radical anionic bpy ligands in **4**.

There are two crystallographically independent molecules in the unit cells of both **3** and **4**. In complex **3**, the diphosphene ligand $[ArP\text{-}PAr]^{2-}$ adopts a *trans* configuration being η^2-coordinated to the Sc center with two Sc−P bonds of 2.661(2) and 2.611(2) Å (or 2.619(2) and 2.658(2) Å). These are appreciably longer than the corresponding bonds found in phosphinidene complex **1** (2.523 Å in average). The P−P bond length (2.194(2) Å or 2.199(2) Å) falls in the range of 2.05−2.21 Å observed for those in the reported transition-metal diphosphene complexes.[10] Although there are some examples of transition-metal diphosphene complexes, to the best of our knowledge, complex **3** is the first example of rare-earth metal derivative. Complex **4** contains two bpy radical-anions ligands, each of them being coordinated to the Sc center via two nitrogen atoms. The Sc center adopts a pseudo-octahedral geometry with six nitrogen atoms occupying the vertices. In agreement with the radical-anion character of the bpy ligand, the C−C bond between two pyridine rings in **4** (1.418(5)−1.438(4) Å) is shorter than in free bpy (1.490(3) Å), and the UV−vis spectrum of **4** in toluene at 25 °C shows a strong absorption around 880 nm (Figure S6).[11] The EPR spectrum of **4** in toluene at 25 °C shows a broad signal with the *g* value of 2.0031 (Figure S7), and the Evans method with **4** in C_6D_6 gives a magnetic moment of 1.40 μ_B at 22 °C. Therefore, there is a spin equilibrium of a singlet state (S = 0) and a triplet state (S = 1) as that observed in $[\{\eta^5\text{-}C_5H_4(CH_2)_2N(CH_3)_2\}\text{-}Sc^{III}(bpy^{\bullet-})_2]$.[11b,e]

Although there are many trivalent rare-earth metal complexes, only very few of them, such as $[(C_5Me_5)_2(THF)\text{-}Ln]_2(\mu\text{-}\eta^2\text{:}\eta^2\text{-}N_2)$,[12] $(C_5Me_5)_3Sm$[13] and several rare-earth metal hydrides,[14] have the ability to undergo reduction. As the most stable oxidation state of rare-earth metal ions is +3, their reductive reactivity can only involve either N_2 loss, pentamethylcyclopentadienyl ligand coupling, or hydride ligand coupling. The reaction between **1** and bpy thus stimulated our interest in exploring more the redox chemistry of **1**. Interestingly, **1** is able to reduce elemental selenium and even elemental tellurium.[15] The reaction of **1** with 1 equiv of selenium or tellurium in toluene at room temperature gave either a Sc diphosphene selenide complex $[(LSc)_2(\mu\text{-Se})(\mu\text{-}\eta^2\text{:}\eta^2\text{-(ArP-PAr)})]$ (**5**) or a Sc diphosphene telluride complex $[(LSc)_2(\mu\text{-Te})(\mu\text{-}\eta^2\text{:}\eta^2\text{-(ArP-PAr)})]$ (**6**) in 51% or 60% yield, respectively (Scheme 4). Once again, in these reactions, two $[PAr]^{2-}$ are oxidatively coupled, and elemental selenium (or

Scheme 4. Reactions of Complex 1 with Se and Te

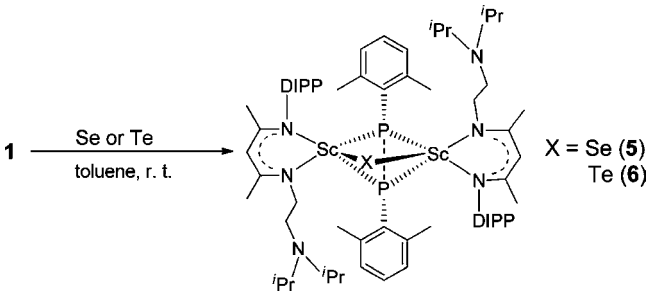

dx.doi.org/10.1021/ja406413d | J. Am. Chem. Soc. 2013, 135, 14784−14796

tellurium) is reduced to Se^{2-} (or Te^{2-}). Complex **1** also reacted rapidly with elemental sulfur (S_8) to give a complicated mixture.

Reaction of **1** with trimethylphosphine sulfide ($Me_3P{=}S$), triphenylphosphine sulfide ($Ph_3P{=}S$), and triphenylphosphine selenide ($Ph_3P{=}Se$) was also studied. Monitoring the reaction of **1** with 1 equiv of $Me_3P{=}S$ by NMR spectroscopy revealed that **1** was almost completely converted into a Sc diphosphene sulfide complex $[(LSc)_2(\mu\text{-}S)(\mu\text{-}\eta^2{:}\eta^2\text{-}(ArP\text{-}PAr))]$ (**7**) at room temperature in 15 min with concomitant formation of PMe_3 (δ = −62 ppm in ^{31}P NMR spectrum). A scaled-up reaction in toluene leads to complex **7** in 48% isolated yield (Scheme 5).

Scheme 5. Reactions of Complex 1 with $R_3P{=}E$ (R = Me or Ph; E = S or Se)

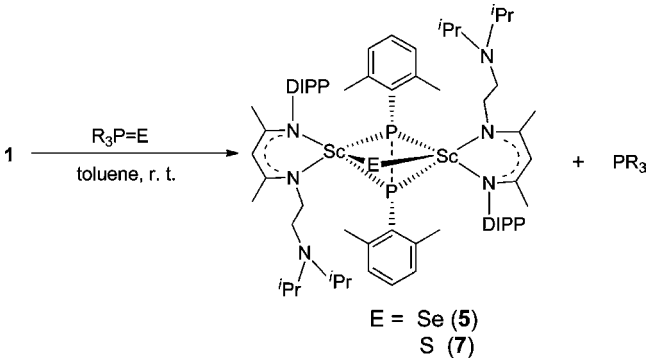

The ^1H NMR spectroscopy monitoring of the reaction of **1** with 1 equiv of $Ph_3P{=}S$ or $Ph_3P{=}Se$ revealed that **1** was almost completely converted into the diphosphene sulfide complex (**7**) or the diphosphene selenide complex $[(LSc)_2(\mu\text{-}Se)(\mu\text{-}\eta^2{:}\eta^2\text{-}(ArP\text{-}PAr))]$ (**5**) at room temperature with concomitant formation of PPh_3 (δ = −5.3 ppm in ^{31}P NMR spectrum). In these reactions, the oxidative coupling of two $[PAr]^{2-}$ in **1** leads to the two-electron reduction of $R_3P{=}E$ (E = S or Se), yielding E^{2-} and PR_3.

The ^{31}P NMR spectra of **5**−**7** exhibit a singlet at δ = −72.2, −60.1, and −79.0 ppm, respectively, revealing the symmetrical structure of all complexes in solution. Complexes **5**−**7** were also structurally characterized by single-crystal X-ray diffraction. These three complexes show similar structural features, the molecular structure of **5** is shown in Figure 3, whereas those of **6** and **7** are given in Figures S1 and S2. In **5**−**7**, the $\mu\text{-}X^{2-}$ (X = Se, Te, or S) ligand bridges two Sc centers, and the diphosphene ligand adopts a *cis* configuration with an η^2-P, P coordination mode to two Sc centers. The Sc−X−Sc angle decreases when the X atom size is increased (91.99(3)°, 86.21(2)°, and 83.10(2)° for complexes **7**, **5**, and **6**, respectively). The Sc−P and P−P bond lengths of these complexes are very close (2.622(1)−2.668 (1) Å and 2.245(1)−2.273(1) Å, respectively).

This spectacular reactivity of **1**, and in particular the formation of the P−P bond, led us to investigate in more detail the bonding situation of complex **1**. For that purpose, DFT calculations were carried out at the B3PW91 level of theory. For the scandium atoms we have used the corresponding RECP (denoted as SDDALL) basis set augmented by an extra *f*-polarization function, when for the rest atoms the widely used 6-31G(d,p) was used. Geometry optimization was performed without any symmetry restriction (see SI). The optimized structure matches well with the experimental one with two nearly equivalent Sc−P bonds (2.516 and 2.534 Å in good agreement with the experimental ones 2.522(1) and 2.528(1) Å, or 2.517(1), and 2.524(1) Å). The P−P distance of 3.556 Å is close to the sum of the van der Waals radii (3.600 Å), and thus the presence of a possible P−P interaction in the complex was investigated. First the molecular orbitals were analyzed, as in a previous study on scandium phophinidene complexes Mindiola and co-workers have reported those ones.[7c] Careful inspection of the molecular orbitals has revealed the five orbitals that describe the bonding of the phosphinidene ligands in the complex (Figure 4).

In addition to the two Sc−P−Sc three-center/two-electron orbitals, π and π^* P−P interactions as well as the antibonding σ P−P are found. This clearly indicates that there is no residual interaction between the two phosphorus atoms in the bimetallic complex. This is further highlighted by other density analysis. Indeed, neither NBO analysis (even at the second-order level) nor the Wiberg index (0.036) revealed any substantial interaction between the two phosphorus atoms, ruling out

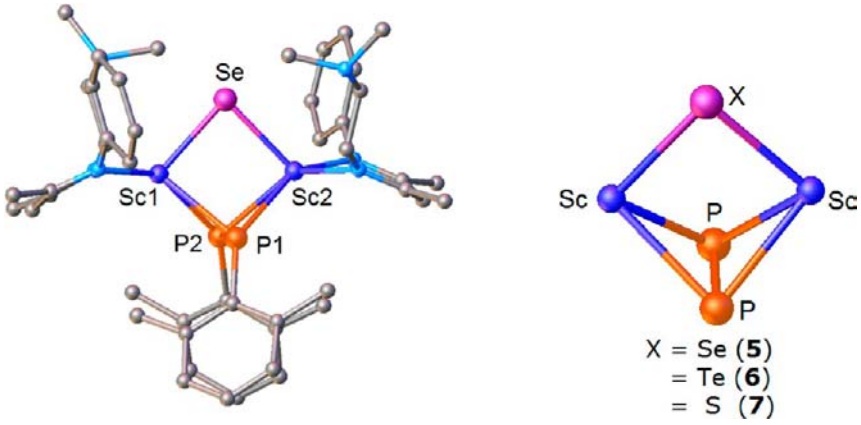

Figure 3. Molecular structure of **5** and heavy atom core of **5**−**7**. Isopropyl groups on the amino arm are represented by only one carbon atom; isopropyl groups of the arene, all H-atoms, and solvents in the lattice are omitted for clarity. Selected metrical parameters (distances in angstroms; angles in degrees): Sc1−Se = 2.543(1), Sc2−Se = 2.545(1), Sc1−P1 = 2.652(1), Sc1−P2 = 2.637(1), P1−P2 = 2.245(1), Sc2−P1 = 2.623(1), Sc2−P2 = 2.651(1); Sc1−Se−Sc2 = 86.21(2), Sc1−P1−Sc2 = 82.45(2), Sc1−P2−Sc2 = 82.20(2), P1−Sc1−P2 = 50.24(2), Se−Sc1−P1 = 89.74(2), Se−Sc1−P2 = 90.56(2).

dx.doi.org/10.1021/ja406413d | J. Am. Chem. Soc. 2013, 135, 14784−14796

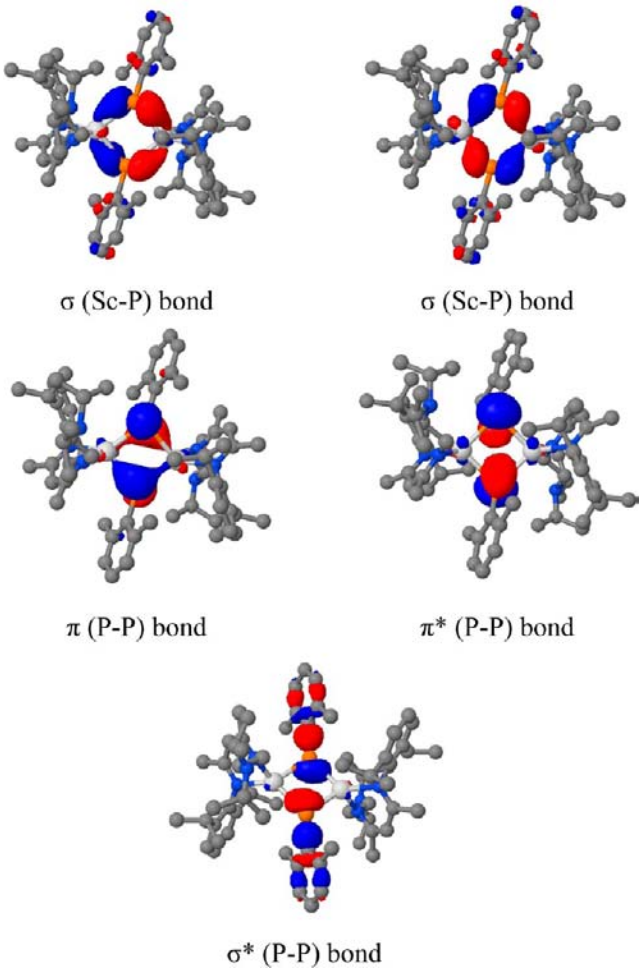

Figure 4. Key molecular orbitals involving the phosphinidene ligand.

the preformation of a P−P bond in complex **1** and indicating that the formal oxidation state of Sc ion is +3.

Addition Chemistry of the Scandium Phosphinidene Complex. Complex **1** undergoes nucleophilic addition reactions with unsaturated substrates, such as allene, nitrile, isocyanide, and CS_2, to give interesting organophosphorous ligands and the corresponding Sc complexes, as shown in Scheme 6. Monitoring the reaction of **1** with benzylallene at room temperature in C_6D_6 by ^1H NMR spectroscopy showed that about 50% of **1** was converted into a new complex **8** in 4 h when 1 equiv of substrate was used. When the amount of benzylallene was increased up to 2 equiv, **1** was almost completely converted into **8** in 6 h. A subsequent scaled-up reaction in toluene provided **8** in 56% yield. On the other hand, reaction of **1** with 2 equiv of benzonitrile was completed within 10 min at room temperature, affording complex **9** in 84% yield. Reaction with 2 equiv of *tert*-butyl isocyanide in 5 h gave complex **11** in 69% yield. The ^1H NMR spectral monitoring of the reaction showed that complex **1** reacted rapidly with 1 equiv of *tert*-butyl isocyanide to provide a monoaddition product **10**, which was isolated at room temperature in 81% yield. Further addition of a second equiv of *tert*-butyl isocyanide to **10** resulted in the formation of complex **11** (Scheme 6). Also, reaction of **1** with 2 equiv of CS_2 rapidly produced complex **12** in high yield. Complexes **8**−**12** were all characterized by single-crystal X-ray diffraction. The molecular

Scheme 6. Reactions of Complex 1 with $PhCH_2CH{=}C{=}CH_2$, PhCN, ^{t}BuNC, and CS_2

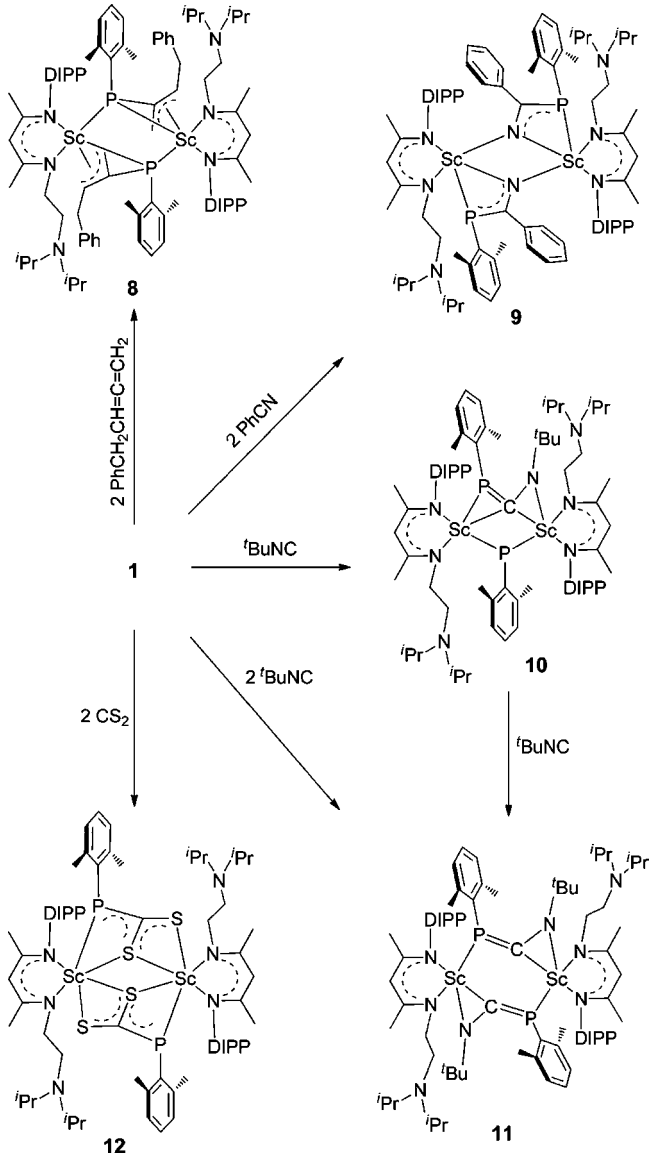

structures of **8**, **9**, and **12** are given in Figures S3−S5, whereas those of **10** and **11** are shown in Figure 5.

In particular the C≡N bond insertion of *tert*-butyl isocyanide into the Sc−P bond gives a novel 1-aza-3-phosphaallyl dianion, that could be described with three different resonance forms, **A**, **B**, and **C** (Scheme 7). In **10**, the C−N and C−P bond lengths of the 1-aza-3-phosphaallyl dianion, 1.324(2) and 1.727(2) Å, are between those of typical single and double bonds. This dianion coordinates to two Sc centers in a μ:η^2-N,C η^2 -C,P-fashion. The Sc2−N7 bond length (2.057 (2) Å) falls in the range of 2.00−2.07 Å observed for Sc−N bonds in the Sc anilido complexes,[9,16] and the Sc1−P1 bond length (2.524 (1) Å) is close to the Ln−P bond lengths in the rare-earth metal−phosphido complexes if the difference in metal ion radii is counted.[17] The Sc1−C67 bond is longer than the Sc2−C67 bond, 2.524 (2) vs 2.406 (2) Å, and both are significantly longer than those in the Sc alkyl complexes (2.19−2.31 Å).[18] On the basis of these structural features, as well as on the calculated natural charges and Wiberg

dx.doi.org/10.1021/ja406413d | J. Am. Chem. Soc. 2013, 135, 14784−14796

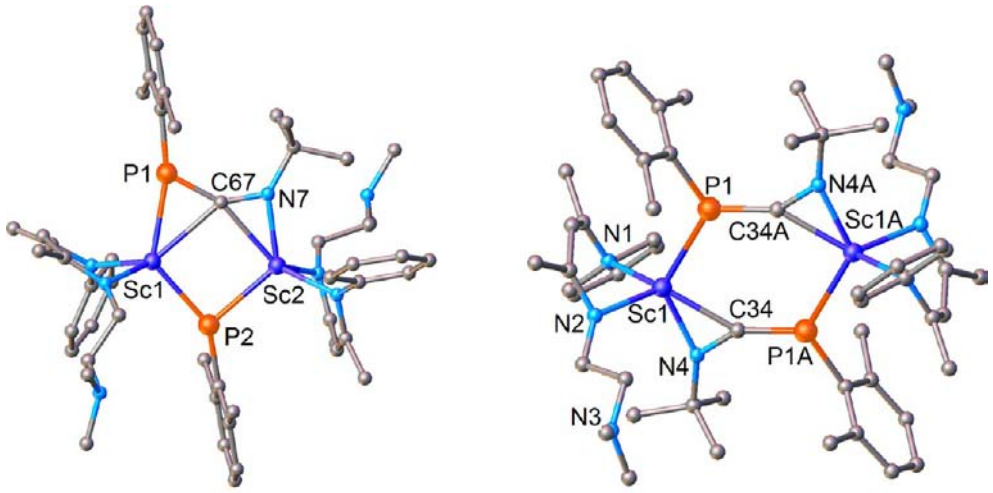

Figure 5. Molecular structures of **10** and **11**. Isopropyl groups on the amino arm are represented by only one carbon atom; isopropyl groups on the arene and all H-atoms are omitted for clarity. Selected metrical parameters (distances in angstroms; angles in degrees) for **10**: Sc1−P1 = 2.524(1), Sc1−P2 = 2.416(1), Sc1−C67 = 2.524(2), Sc2−N7 = 2.057(2), Sc2−P2 = 2.519(1), Sc2−C67 = 2.406(2), C67−P1 = 1.727(2), C67−N7 = 1.324(2); P1−C67−N7 = 141.41(14), Sc1−C67−Sc2 = 89.88(6), Sc1−C67−P1 = 69.98(6), Sc2−C67−N7 = 58.70(9), Sc1−P2−Sc2 = 89.77(2). For **11**: Sc1−N1 = 2.143(2), Sc1−N2 = 2.132(2), Sc1−N4 = 2.062(2), Sc1−P1 = 2.630(1), Sc1−C34 = 2.182(2), C34−N4 = 1.316(2), C34−P1 = 1.718(2); N4−C34−Sc1 = 67.00(9), Sc1−C34−P1A = 147.5(1), N4−C34−P1A = 145.50(14).

Scheme 7. Three Resonance Forms of 1-aza-3-Phosphaallyl Dianion

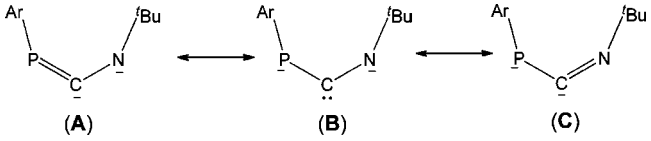

bond orders, the 1-aza-3-phosphaallyl dianion of **10** is best described by the resonance form **A** (Scheme 8).

Unlike complex **10**, complex **11** contains two 1-aza-3-phosphaallyl dianions and is a centrosymmetric dimer. The C34−N4 and C34−P1 bond lengths of the 1-aza-3-phosphaallyl dianion in **11** are 1.316(2) and 1.718(2) Å, respectively, which are close to those in **10**. However, the central carbon atom of the dianion only coordinates to one Sc ion, and this can be ascribed to an expansion in coordination ring caused by the replacement of a phosphinidene ligand with a 1-aza-3-phosphaallyl dianion. This is also confirmed by Wiberg bond order analysis, which predicts an almost zero bond order (0.05) for Sc1−C34A, while it was 0.33 for the corresponding bond in model complex **10m** (Scheme 8). The Sc1−C34 bond (2.182(2) Å) is much shorter than that of **10**. The Sc1−N4 bond (2.062(2) Å) is close to that of **10**, whereas

Scheme 8. Selected Natural Charges and Wiberg Bond Orders for Model Compounds 10m and 11m

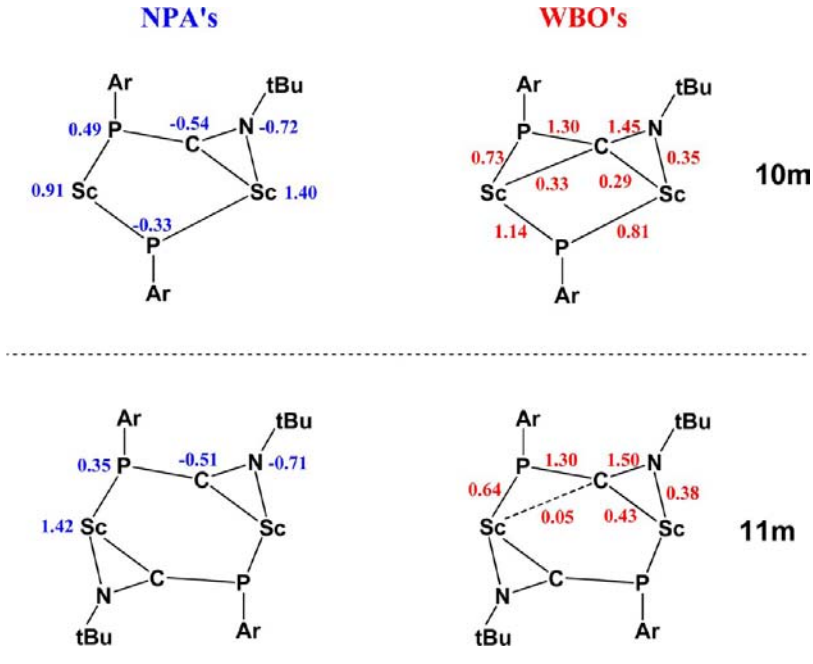

dx.doi.org/10.1021/ja406413d | J. Am. Chem. Soc. 2013, 135, 14784−14796

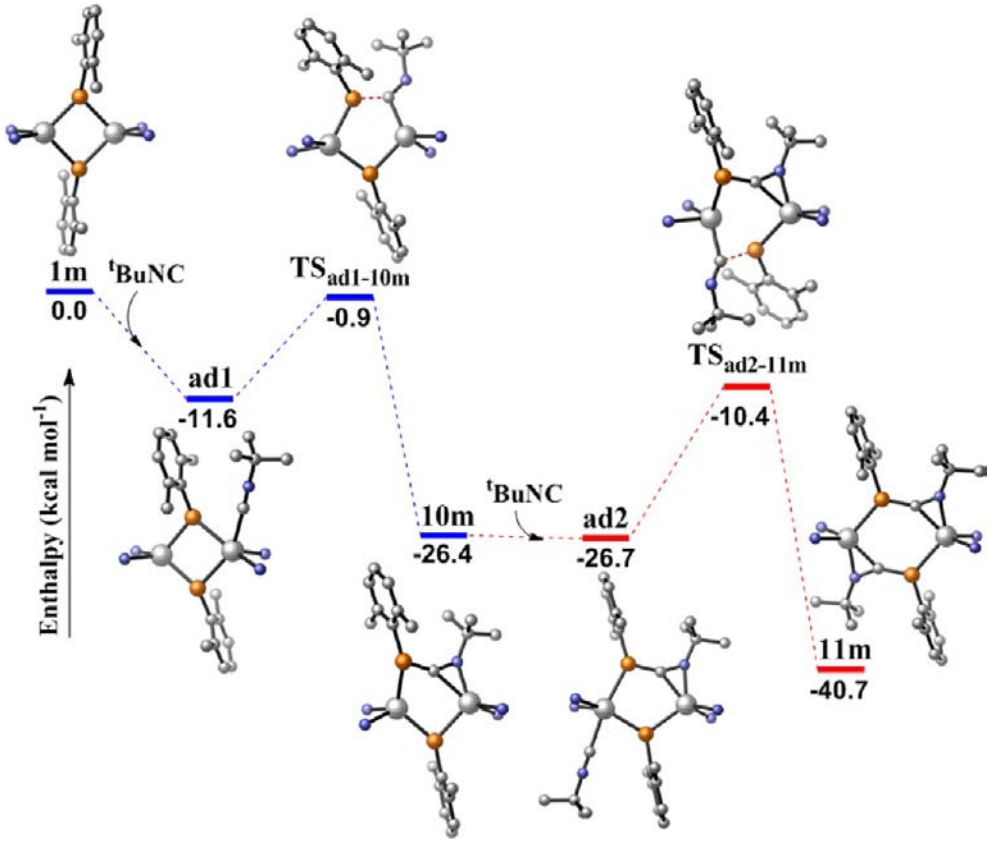

Figure 6. Plausible energy profile for the reaction of **1m** with one and two equivalents of ^{t}BuNC to afford complexes **10m** and **11m**, respectively.

the Sc1−P1 bond (2.630 (1) Å) is significantly longer. The previous analysis in conjunction with the natural charges clearly shows that the 1-aza-3-phosphaallyl dianion moiety of **11** is best described again as in the case of **10** with the resonance form **A**.

The formation of complexes **10** and **11** after the addition of 1 or 2 equiv of ^{t}BuNC, respectively, to the precursor complex **1** has been studied computationally at the DFT (B3PW91) level of theory (see SI for computational details). In order to save computational time, due to the relative large size of the system under study, and also to avoid conformational problems, we thus slightly simplified the substituents of the β-diketiminato ligand (that are distant from the active site of the complex) by replacing the *i*-Pr by methyl groups.[19] The reaction begins with the formation of an adduct, **ad1**, in which the C atom of ^{t}BuNC is bonded to one Sc center (with Sc−C distance of 2.329 Å). This coordination is exothermic by 11.6 kcal mol^{-1}. The insertion reaction proceeds from **ad1** with the development of the interaction between the carbon atom of the coordinated ^{t}BuNC moiety and the P atom of the phosphinidene ligand (distance of 1.855 Å). This interaction is further supported by the concomitant lengthening of the Sc−P bond by up to 0.650 Å at the transition state, $\mathbf{TS}_{\mathbf{ad1-10m}}$. It should be noted, that the C−N−$C_{t_{Bu}}$ bond angle is bent by 49.8° with respect to the adduct which is almost linear, indicating a nucleophilic assistance of the nitrogen. This results in an activation barrier of 10.7 kcal mol^{-1} where the corresponding reaction coordinate in $\mathbf{TS}_{\mathbf{ad1-10m}}$ (−49 cm^{-1}) is the motion involving the formation of a P−C bond and leads to experimentally observed intermediate, **10m**. This process is exothermic by 14.8 kcal mol^{-1}, and even more exothermic with respect to the entrance channel (26.4 kcal mol^{-1}). In the second insertion, two pathways are the most probable, either a *cis* or *trans* insertion with respect to the first inserted substrate. In the *trans* insertion, the addition of the second ^{t}BuNC molecule will result in a weak coordinated adduct, **ad2** (stabilization of only 0.3 kcal mol^{-1}). This marginal stabilization, in contrast to the formation of **ad1**, is mainly attributed to the relative strong steric congestion in *trans* position to the first inserted substrate. This is also reflected in the higher activation barrier for the second insertion with respect to the first one, being 16.3 kcal mol^{-1} (Figure 6). Interestingly, this steric hindrance of the β-diketiminato ligand excludes any possibility of subsequent C−C coupling (as well as potential P−P coupling) between the two inserted molecules (all calculations trying to locate such TS remained unsuccessful). Moreover, it is noteworthy that all the attempts to locate a possible transition state for a *cis* insertion (allowing subsequent C−C coupling) failed due to the fact that the β-diketiminato is strongly bent toward the PAr arm leaving no space for the incoming substrate to coordinate and consequently to insert into the Sc−P bond. The outcome of the insertion process is the formation of the experimental product, **11m**, that is strongly stabilized (14.0 kcal mol^{-1}) with respect to the **ad2**, with the overall reaction being exothermic by 40.7 kcal mol^{-1}. Hence, the reaction is thermodynamically favored and kinetically easily accessible in line with the experimental observations.

Reactions of the Scandium Phosphinidene Complex with CO and Mo(CO)$_6$. Most fascinatingly, reaction of **1** with carbon monoxide (1.0 atm) in 15 min at room temperature gave a novel Sc oxide containing 3-oxo-4-ylidene-1,2-diphosphetene ligand (**13**), which was isolated in 53% yield (Scheme 9). The molecular structure is shown in Figure 7. The complex contains two Sc centers, which are in strikingly

dx.doi.org/10.1021/ja406413d | J. Am. Chem. Soc. 2013, 135, 14784−14796

Scheme 9. Reaction of Complex 1 with CO

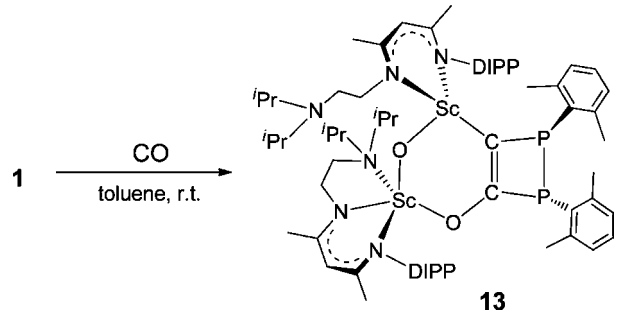

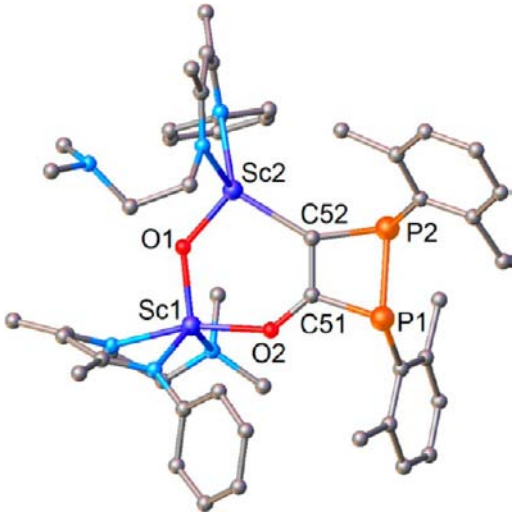

Figure 7. Molecular structure of **13**. Isopropyl groups on the amino arm are represented by only one carbon atom; isopropyl groups on the arene, all H-atoms, and solvents in the lattice are omitted for clarity. Selected metrical parameters (distances in angstroms; angles in degrees): Sc1−O1 = 1.909(2), Sc1−O2 = 1.997(2), Sc2−O1 = 1.879(2), Sc2−C52 = 2.250(2), C51−O2 = 1.322(3), C51−C52 = 1.385(3), C51−P1 = 1.833(2), C52−P2 = 1.855(2), P1−P2 = 2.228(1); O2−Sc1−O1 = 97.63(7), C52−Sc2−O1 = 100.98(8), P1−C51−C52 = 107.0(2), P2−C52−C51 = 97.0(2), P2−P1−C51 = 73.35(8), P1−P2−C52 = 78.55(8).

different environments: one Sc center is coordinated by one oxygen atom of the 3-oxo-4-ylidene-1,2-diphosphetene ligand, three nitrogen atoms of the tridentate nitrogen ligand (L), and a μ-O^{2-} ligand, while the other Sc center is coordinated by one carbon atom of the 3-oxo-4-ylidene-1,2-diphosphetene ligand, two nitrogen atoms of the tridentate nitrogen ligand (L), and a μ-O^{2-} ligand. The C51−P1(1.833(2) Å), C52−P2 (1.855(2) Å), and P1−P2 (2.228(1) Å) bonds of the C2P2 four-membered ring are consistent with single bonds, whereas the C51−C52 (1.385(3) Å) bond reveals double-bond character, indicating a 1,2-diphosphetene structure,[20] with the two 2,6-dimethylphenyl substituents on the phosphorus atoms adopting a *trans* configuration. The solution NMR spectra features of **13** are consistent with the structure revealed by the single crystal X-ray diffraction. In particular, the ^{1}H NMR spectrum shows two sets of signals for two tridentate nitrogen ligands, whereas the ^{31}P NMR spectrum shows two doublets at δ = 38.2 and −46.2 ppm. The formation of **13** is a sequence of steps involving C−P bond formation, C−C coupling, C−O bond cleavage of CO, and P−P coupling.

Complex **1** also reacts with $Mo(CO)_6$. The reaction was completed in 30 min at room temperature and provided a Sc−Mo heterobimetallic complex containing 1,4-diphospha-2-ylidene-3-oxo-buta-1,3-diene ligand (**14**) in 91% yield (Scheme 10). Complex **14** shows remarkable structural differences

Scheme 10. Reaction of Complex 1 with $Mo(CO)_6$

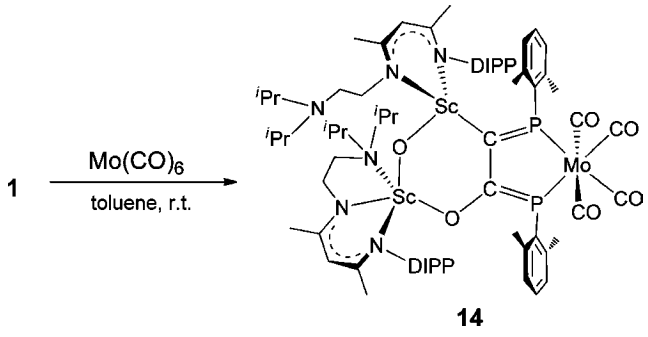

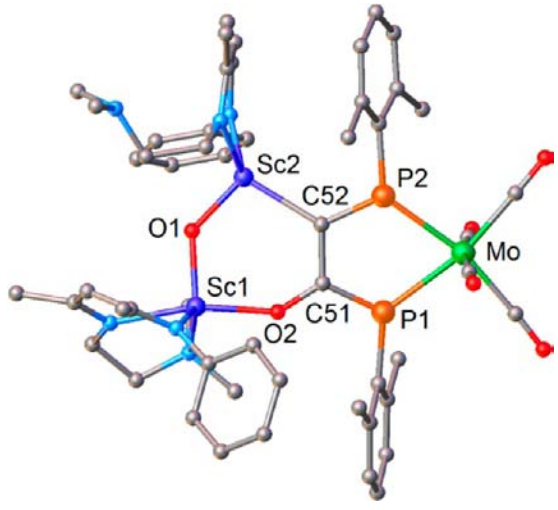

Figure 8. Molecular structure of **14**. Isopropyl groups on the amino arm are represented by only one carbon atom; isopropyl groups on the arene and all H-atoms are omitted for clarity. Selected metrical parameters (distances in angstroms, angles in degrees): Sc1−O1 = 1.899(3), Sc1−O2 = 2.044(3), Sc2−O1 = 1.864(3), Sc2−C52 = 2.288(4), C51−O2 = 1.332(5), C51−C52 = 1.473(6), C51−P1 = 1.726(4), C52−P2 = 1.702(4), Mo−P1 = 2.493(2), Mo−P2 = 2.471(2); O2−Sc1−O1 = 96.5(2), C52−Sc2−O1 = 102.4(2), P1−C51−C52 = 117.3(3), P2−C52−C51 = 113.5(3), Mo−P1−C51 = 115.6(2), Mo−P2−C52 = 119.4(2), P1−Mo−P2 = 73.06(4).

relative to complex **13** (Figure 8). In **14**, the C51−P1 and C52−P2 bonds (1.726(4) and 1.702(4) Å) are significantly shorter than those in **13** (1.833(2) and 1.855(2) Å) and reveal double-bond character, whereas the C51−C52 bond (1.473(6) Å) is longer than that in **13** (1.385(3) Å) and reveals single-bond character. Two phosphorus atoms coordinate to the Mo center with two nonequivalent Mo−P bond lengths of 2.493(2) and 2.471(2) Å, and the P1−P2 separation is larger than 2.95 Å. The phosphorus atoms adopt trigonal planar geometries, allowing the lone pair of each phosphorus atom to become delocalized throughout the C51−C52−P2−Mo−P1 five-membered ring. Consistent with the C−P double bond character, the ^{31}P NMR spectrum of **14** shows two doublets

dx.doi.org/10.1021/ja406413d | J. Am. Chem. Soc. 2013, 135, 14784−14796

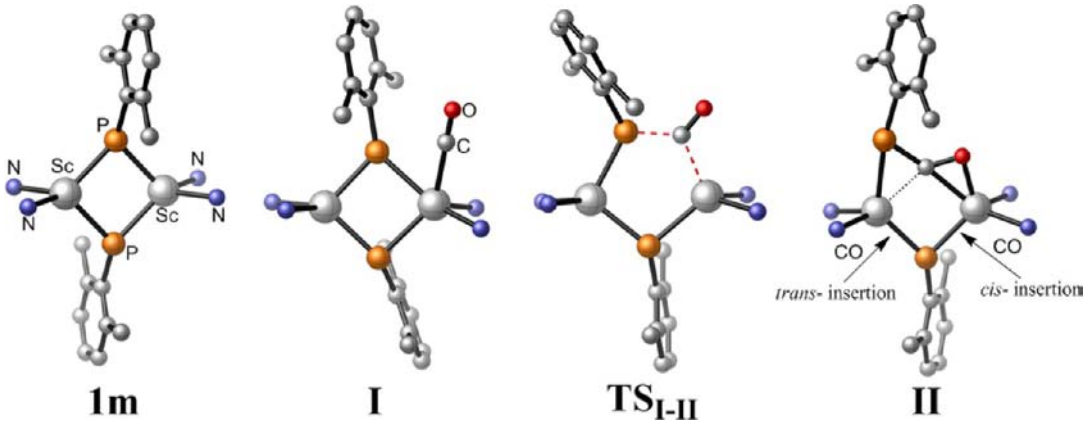

Figure 9. Geometry of the extrema along the pathway for the first CO insertion. Most of the atoms of β-diketiminato ligand and all hydrogen atoms are omitted for clarity.

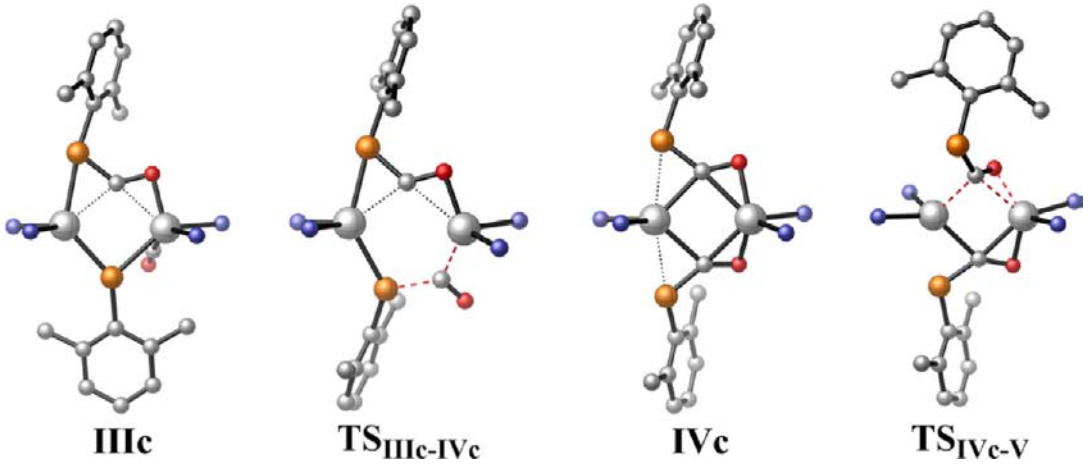

Figure 10. Geometry of the extrema along the pathway for the second CO *cis* insertion and the subsequent isomerization. Most of the atoms of β-diketiminato ligand and all hydrogen atoms are omitted for clarity.

at δ = 300.0 and 85.3 ppm, which are significantly downfield in comparison with those in **13** (δ = 38.2 and −46.2 ppm). It is also noteworthy that complex **13** does not react with $Mo(CO)_6$ at 50 °C in C_6D_6. When the temperature was raised to 75 °C, the reaction slowly occurs to give a complicated mixture, and the formation of complex **14** was not observed.

Computational Studies on the Reaction Mechanism of 1 with CO. Starting from complex **1m** (Figure 9), the formation of the intermediate **II** takes place through insertion of CO into one of the four available Sc−P bonds. Although the insertion of CO into rare-earth metal−P bond is unprecedented, the insertion of CO into rare-earth metal−C bond has been well documented.[21] The activation barrier is 11.4 kcal mol^{-1}, with respect to the adduct **I**. The distance between the inserted CO substrate and the P atom is 1.854 Å, while the Sc−C_{CO} distance in **TS**$_{I-II}$ is 2.215 Å, and the C≡O bond length of the substrate is elongated by 0.099 Å with respect to free CO. Analytical frequency calculation confirmed the nature of **TS**$_{I-II}$ that is characterized by a single imaginary frequency (ν_i = −104 cm^{-1}). The insertion process is predicted to be exothermic by 15.8 kcal mol^{-1}, with respect to the adduct **I**. It should be noted that the activation barrier as well as the exothermicity of this step is energetically similar to the calculated one in the case of the ^{t}BuNC first insertion. The C−O bond in intermediate **II** is further elongated by 0.065 Å with respect to **TS**$_{I-II}$, pointing clearly the structural change that accompanies the reduction of the CO. Moreover, the bonding mode of the CO in intermediate **II** corresponds to a η^2-, with the Sc−C and Sc−O distances being 2.330 and 1.999 Å, respectively.

The subsequent step in the reaction coordinate corresponds to the second addition of CO. As already stated for the second insertion of ^{t}BuNC, the second CO molecule can insert either in *cis* or *trans* position with respect to the first inserted molecule (Figure 9), yielding two isomeric complexes **IVc** and **IVt** shown in Figures 10 and S55, respectively. As mentioned for ^{t}BuNC, only the *cis* orientation allows subsequent C−C and P−P coupling, due to steric effects. Unlike the ^{t}BuNC insertion, the transition state leading to the formation of intermediate **IVc** has been located on the potential energy surface, **TS**$_{IIIc-IVc}$.

Hence, the second insertion in *cis* fashion leads to the lengthening of the C−O bond in **IVc** with respect to free monoxide molecule by 0.165 Å, being 1.302 Å. At **TS**$_{IIIc-IVc}$, the incoming CO molecule lies in the same plane as the Sc−P−C−P−Sc atoms, being in close resemblance with **TS**$_{I-II}$ one. The activation barrier for this process is low (12.5 kcal mol^{-1}), while the formation of intermediate **IVc** is predicted to be exothermic by 11.2 kcal mol^{-1}. An isomerization of complex **IVc** is thus required to allow the subsequent C−C coupling and involves a rotation of one of the two C═O bonds. This can be achieved by passing via an almost barrierless transition state, **TS**$_{IVc-V}$, (barrier of only 2.2 kcal mol^{-1}). At this transition state, both CO interacts in a μ:η:η^2 fashion with each metal (Figure 10). In

dx.doi.org/10.1021/ja406413d | J. Am. Chem. Soc. 2013, 135, 14784−14796

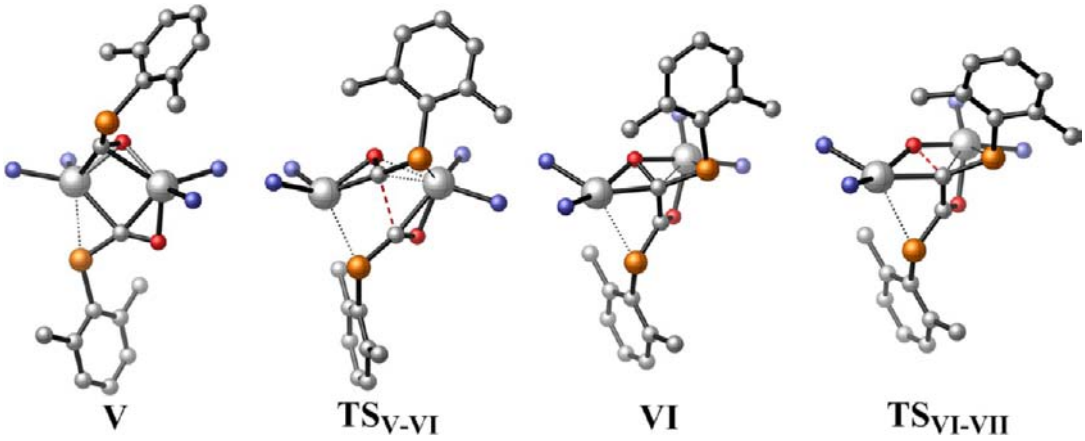

Figure 11. Geometry of the extrema along the pathway for the C−C coupling and C−O cleavage. Most of the atoms of β-diketiminato ligand and all hydrogen atoms are omitted for clarity.

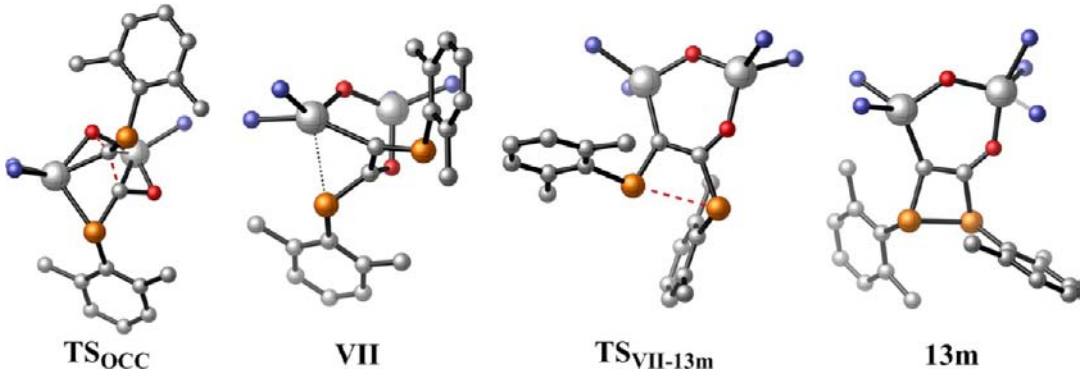

Figure 12. Geometry of the extrema along the pathway for the P−P coupling. Most of the atoms of β-diketiminato ligand and all hydrogen atoms omitted for clarity.

the resulting intermediate **V** (Figure 11), there is a change of coordination mode for one CO moiety that becomes μ:μ:η^2. For the μ:μ:η^2 CO moiety, the C−Sc and O−Sc bonds are 2.158 and 2.145 Å long, respectively, whereas for the μ:η:η^2 CO, the C−Sc and O−Sc distances are 2.481 and 2.145 Å. The μ:μ:η^2 C═O bond is thus lengthened by 0.064 Å. Instead of the insertion of a second CO molecule, we have also considered the direct C_{CO}−P coupling from complex **II** (cf. Figure S56). The corresponding transition state, **TS$_{C-P}$**, adopts a butterfly-like geometry, with the Sc−P−Sc−C torsion angle being −42.6°. This kind of geometrical variation is essential for the C−P coupling in order to proceed. However, the latter has a huge impact on the activation barrier being 29.6 kcal mol^{-1}, and the high endothermicity of the reaction (30 kcal mol^{-1}) with respect to **II** excludes any possibility for the existence of such pathway.

After the second CO insertion and isomerization, the subsequent step of the mechanism corresponds to the C−C coupling between the ArPCO fragments (Figure 11). The activation barrier is computed to be relatively low (22.7 kcal mol^{-1}), and the step is exothermic by 3.7 kcal mol^{-1}. At **TS$_{V-VI}$**, the O−C−C−O dihedral angle is 37.4°, and the C−C bond distance to be formed is still long (2.301 Å). The two CO bond distances are different (1.279 and 1.355 Å) with the latter being in a bridging position, which explains the observed lengthening of the corresponding bond.

The next step of the reaction path involves the cleavage of the bridging CO bond (Figure 11) through transition state **TS$_{VI-VII}$** and yielding the μ-oxo intermediate **VII** with a very low activation barrier of 3.3 kcal mol^{-1}. The low activation barrier of this step is mainly due to the fact that the μ:η^2-CO moiety is already strongly activated. Indeed, no significant geometrical changes are observed compared to the intermediate **VI**. Insomuch that the shape of geometries are close, with the length of the C−O bond (1.821 Å), which is going to be broken in **TS$_{VI-VII}$**, being only 0.033 Å longer than that in intermediate **VI**. Indeed, the previously formed C−C bond length remains almost the same in the two structures (difference of 0.016 Å). Also, the bond distances between the η^2-carbon with the scandium centers in the transition state differ by 0.1 Å with that of intermediate **VI**, being also true for the analogous η^1-C−Sc bonds. The imaginary frequency of **TS$_{VI-VII}$**, ν_i = 289 cm^{-1}, involves the cleavage of the μ:η^2-CO bond. Thus, this transition state could be characterized as an early transition state, as shown above (Figure 11). It should also be noted that we have also located a transition state (denoted as **TS$_{OCC}$** in Figure 12) which corresponds to a simultaneous C−O bond cleavage and C−C coupling. The high activation barrier of 38.9 kcal mol^{-1} with respect to intermediate **V** prevents from any further consideration.

In the final step, the P−P coupling occurs to form complex **13m.** This process is highly exothermic (34.0 kcal mol^{-1}) with an activation barrier of 19.7 kcal mol^{-1}. This indicates that the formed P−P bond is rather strong. In the vibrational mode corresponding to the imaginary frequency of **TS$_{VII-13m}$**, ν_i = 593 cm^{-1}, the dominant motions involve the elongation of the

dx.doi.org/10.1021/ja406413d | J. Am. Chem. Soc. 2013, 135, 14784−14796

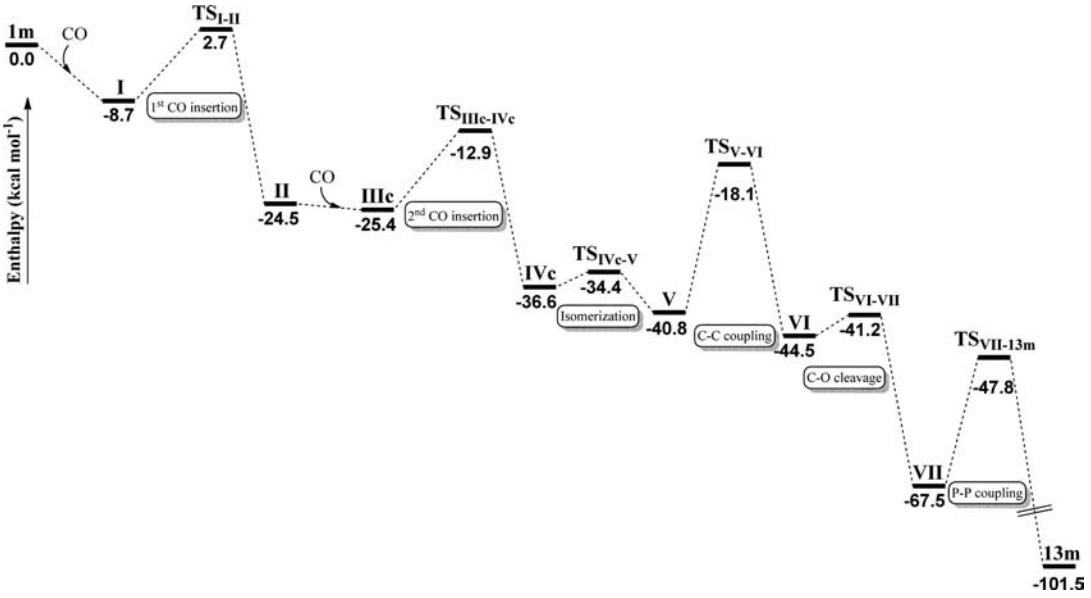

Figure 13. Enthalpy energy profile for the reaction of **1m** with two equivalents of CO to afford complex **13m**.

two C−P bonds and the simultaneous decrease of the C−C and P−P bond lengths. In complex **13m** the torsion angle is computed to be 20.3° in very close agreement with the experimentally observed 18.8(2)°. To summarize this rather complicated reactivity study, a plausible mechanism including all the aforementioned steps is depicted schematically in Figure 13. As can be seen, the reaction is a downhill process where the rate-determining step is the C−C coupling where the barrier is however rather low (around 23.0 kcal mol^{-1}) in line with a rapid reaction. The latter can be ascribed to the difficulty to homocouple two negatively charged carbons of each OCPAr moiety.

3. CONCLUSION

The study on a four-coordinate scandium bridged phosphinidene complex, $[LSc(\mu\text{-}PAr)]_2$ (L = (MeC(NDIPP)CHC(Me)-($NCH_2CH_2N(^iPr)_2$)), DIPP = 2,6-$(^iPr)_2C_6H_3$; Ar = 2,6-$Me_2C_6H_3$) (**1**), revealed rich reactivity with formation of interesting phosphorus-containing molecules. Distinct from other transition-metal bridged phosphinidene complexes of type **E** (Chart 1)[4] as well as from the five-coordinate Sc bridged phosphinidene complexes supported by PNP ligand $[(PNP)\text{-}Sc(\mu\text{-}PAr)]_2$ (Ar = 2,4,6-$^iPr_3C_6H_2$),[7c] which are showing sluggish reactivity, complex **1** is highly reactive toward various substrates. It reacts with a Lewis base as 4-dimethylamino pyridine (DMAP) to form a DMAP coordinated Sc phosphinidene complex $[LSc(DMAP)(\mu\text{-}PAr)]_2$. Also, complex **1** has spectacular redox reactivity and is able to reduce not only 2,2′-bipyridine, phosphine sulfide, and phosphine selenide but also elemental selenium and elemental tellurium. This associated oxidative formation of the P−P bond occurs during the reaction, since DFT calculations do not reveal any preformed bond in **1**. Complex **1** also easily undergoes nucleophilic addition reactions with unsaturated substrates, such as benzylallene, benzonitrile, *tert*-butyl isocyanide, and CS_2. Furthermore, this complex initiates the homologation of CO and the coordinated CO. The observed high reactivity of this four-coordinate Sc bridged phosphinidene complex is likely to be due to the mismatched scandium−phosphinidene coordination and the coordinatively unsaturated feature. DFT studies were carried out to give insights on the reactivity of complex **1** with two different substrates, involving insertion onto the Sc−P bonds. Furthermore, it was possible to determine a plausible sequence of reaction to lead to a C_2P_2 ring from CO insertion. In particular, the reactivity begins by two distinct insertions of CO, followed by a C−C coupling. From this coupled intermediate, a C−O bond cleavage occurs, leading to subsequent P−P coupling reaction. The C−C coupling, that involves two anions, is predicted to be the rate determining step of the reaction.

■ ASSOCIATED CONTENT

Ⓢ Supporting Information

Experimental and computational details; CIF file giving X-ray crystallographic data for **1**−**14**. These materials are available free of charge via the Internet at http://pubs.acs.org.

■ AUTHOR INFORMATION

Corresponding Authors

laurent.maron@irsamc.ups-tlse.fr
yaofchen@mail.sioc.ac.cn

Notes

The authors declare no competing financial interest.

■ ACKNOWLEDGMENTS

This work was supported by the National Natural Science Foundation of China (grant nos. 21072209, 21132002 and 21121062), the State Key Basic Research & Development Program (grant no. 2012CB821600), Shanghai Municipal Committee of Science and Technology (10DJ1400104), and Chinese Academy of Sciences. L.M. is member of the Institut Universitaire de France. CalMip and Cines are acknowledged for a generous grant of computing time. The Humboldt foundation is also acknowledged.

■ REFERENCES

(1) For some representative reviews, see: (a) Cowley, A. H. *Acc. Chem. Res.* **1997**, *30*, 445. (b) Stephan, D. W. *Angew. Chem., Int. Ed.* **2000**, *39*, 314. (c) Mathey, F. *Angew. Chem., Int. Ed.* **2003**, *42*, 1578. (d) Lammertsma, K. *Top. Curr. Chem.* **2003**, *229*, 95. (e) Greenberg,

S.; Stephan, D. W. *Chem. Soc. Rev.* **2008**, *37*, 1482. (f) Waterman, R. *Dalton Trans.* **2009**, 18. (g) Aktaş, H.; Slootweg, J. C.; Lammertsma, K. *Angew. Chem., Int. Ed.* **2010**, *49*, 2102.

(2) (a) Alvarez, C. M.; Alvarez, M. A.; García, M. E.; González, R.; Ruiz, M. A.; Hamidov, H.; Jeffery, J. C. *Organometallics* **2005**, *24*, 5503. (b) Alvarez, M. A.; García, M. E.; González, R.; Ruiz, M. A. *Organometallics* **2008**, *27*, 1037. (c) Alvarez, M. A.; García, M. E.; González, R.; Ramos, A.; Ruiz, M. A. *Organometallics* **2010**, *29*, 1875. (d) Alvarez, M. A.; García, M. E.; González, R.; Ramos, A.; Ruiz, M. A. *Organometallics* **2011**, *30*, 1102. (e) Alvarez, M. A.; García, M. E.; González, R.; Ruiz, M. A. *Organometallics* **2010**, *29*, 5140. (f) Alvarez, M. A.; García, M. E.; González, R.; Ruiz, M. A. *Organometallics* **2011**, *50*, 7894. (g) Alvarez, M. A.; García, M. E.; González, R.; Ramos, A.; Ruiz, M. A. *Inorg. Chem.* **2011**, *50*, 7894. (h) Alvarez, C. M.; Alvarez, M. A.; García, M. E.; González, R.; Ramos, A.; Ruiz, M. A. *Inorg. Chem.* **2011**, *50*, 10937. (i) Alvarez, M. A.; García, M. E.; González, R.; Ruiz, M. A. *Dalton Trans.* **2012**, *41*, 14498.

(3) (a) Alvarez, M. A.; Amor, I.; García, M. E.; García-Vivó, D.; Ruiz, M. A. *Inorg. Chem.* **2007**, *46*, 6230. (b) Alvarez, M. A.; García, M. E.; Ruiz, M. A.; Suárez, J. *Angew. Chem., Int. Ed.* **2011**, *50*, 6383. (c) Alvarez, M. A.; Amor, I.; García, M. E.; García-Vivo, D.; Ruiz, M.; Suárez, J. *Organometallics* **2012**, *31*, 2749. (d) Alvarez, M. A.; Amor, I.; García, M. E.; García-Vivó, D.; Ruiz, M.; Suárez, J. *Organometallics* **2010**, *29*, 4384.

(4) (a) Huttner, G.; Evertz, K. *Acc. Chem. Res.* **1986**, *19*, 406. (b) Graham, T. W.; Udachin, K. A.; Carty, A. J. *Chem. Commun.* **2005**, 4441. (c) Graham, T. W.; Udachin, K. A.; Carty, A. J. *Chem. Commun.* **2006**, 2699. (d) Graham, T. W.; Udachin, K. A.; Carty, A. J. *Inorg. Chim. Acta* **2007**, *360*, 1376. (e) Scheer, M.; Himmel, D.; Kuntz, C.; Zhan, S.; Leiner, E. *Chem.—Eur. J.* **2008**, *14*, 9020. (f) Scheer, M.; Kuntz, C.; Stubenhofer, M.; Zabel, M.; Timoshkin, A. Y. *Angew. Chem., Int. Ed.* **2010**, *49*, 188.

(5) (a) García, M. E.; Riera, V.; Ruiz, M. A.; Sáez, D.; Vaissermann, J.; Jeffery, J. C. *J. Am. Chem. Soc.* **2002**, *124*, 14304. (b) Amor, I.; García, M. E.; Ruiz, M. A.; Sáez, D.; Hamidov, H.; Jeffery, J. C. *Organometallics* **2006**, *25*, 4857.

(6) (a) Pearson, R. G. *Hard and Soft Acids and Bases*; Dowden, Hutchinson and Ross: Stroudsburg, PA, 1973; (b) Jensen, W. B. *The Lewis Acid-Base Concepts: An Overview*; John Wiley and Sons: Hoboken, NJ, 1980.

(7) (a) Masuda, J. D.; Jantunen, K. C.; Ozerov, O. V.; Noonan, K. J. T.; Gates, D. P.; Scott, B. L.; Kiplinger, J. L. *J. Am. Chem. Soc.* **2008**, *130*, 2408. (b) Cui, P.; Chen, Y. F.; Xu, X.; Sun, J. *Chem. Commun.* **2008**, 5547. (c) Wicker, B. F.; Scott, J.; Andino, J. G.; Gao, X. F.; Park, H.; Pink, M.; Mindiola, D. J. *J. Am. Chem. Soc.* **2010**, *132*, 3691. (d) Cui, P.; Chen, Y. F.; Borzov, M. V. *Dalton Trans.* **2010**, *39*, 6886. (e) Lv, Y. D.; Xu, X.; Chen, Y. F.; Leng, X. B.; Borzov, M. V. *Angew. Chem., Int. Ed.* **2011**, *50*, 11227.

(8) Xu, X.; Xu, X. Y.; Chen, Y. F.; Sun, J. *Organometallics* **2008**, *27*, 758.

(9) Lu, E. L.; Li, Y, X.; Chen, Y. F. *Chem. Commun.* **2010**, *46*, 4469.

(10) (a) Vahrenkamp, H.; Wolters, D. *Angew. Chem., Int. Ed. Engl.* **1983**, *22*, 154. (b) Fenske, D.; Merzweiler, K. *Angew. Chem., Int. Ed. Engl.* **1986**, *25*, 338. (c) Cowley, A. H.; Giolando, D. M.; Nunn, C. M.; Pakulski, M.; Westmoreland, D.; Norman, N. C. *J. Chem. Soc., Dalton Trans.* **1988**, 2127. (d) Ho, J. W.; Breen, T. L.; Ozarowski, A.; Stephan, D. W. *Inorg. Chem.* **1994**, *33*, 865. (e) Etkin, N.; Benson, M. T.; Courtenay, S.; McGlinchey, M. J.; Bain, A. D.; Stephan, D. W. *Organometallics* **1997**, *16*, 3504. (f) Xin, S. X.; Woo, H. G.; Harrod, J. F.; Samuel, E.; Lebuis, A.-M. *J. Am. Chem. Soc.* **1997**, *119*, 5307. (g) Burrows, A. D.; Dransfeld, A.; Green, M.; Jeffery, J. C.; Jones, C.; Lynam, J. M.; Nguyen, M. T. *Angew. Chem., Int. Ed.* **2001**, *40*, 3221.

(11) (a) Schultz, M.; Boncella, J. M.; Berg, D. J.; Tilley, T. D.; Andersen, R. A. *Organometallics* **2002**, *21*, 460. (b) Beetstra, D. J.; Meetsma, A.; Hessen, B.; Teuben, J. H. *Organometallics* **2003**, *22*, 4372. (c) Tupper, K. A.; Tilley, T. D. *J. Organomet. Chem.* **2005**, *690*, 1689. (d) Williams, B. N.; Huang, W. L.; Miller, K. L.; Diaconescu, P. L. *Inorg. Chem.* **2010**, *49*, 11493. (e) Scarborough, C. C.; Wieghardt, K. *Inorg. Chem.* **2011**, *50*, 9773.

(12) (a) Evans, W. J.; Lee, D. S.; Ziller, J. W.; Kaltsoyannis, N. *J. Am. Chem. Soc.* **2006**, *128*, 14176. (b) Schmiege, B. M.; Ziller, J. W.; Evans, W. J. *Inorg. Chem.* **2010**, *49*, 10506.

(13) Evans, W. J.; Forrestal, K. J.; Ziller, J. W. *J. Am. Chem. Soc.* **1998**, *120*, 9273.

(14) (a) Piers, W. E.; Ferguson, G.; Gallagher, J. F. *Inorg. Chem.* **1994**, *33*, 3784. (b) Evans, W. J.; Schmiege, B. M.; Lorenz, S. E.; Miller, K. A.; Champagne, T. M.; Ziller, J. W.; DiPasquale, A. G.; Rheingold, A. L. *J. Am. Chem. Soc.* **2008**, *130*, 8555. (c) Lu, E. L.; Chen, Y. F.; Leng, X. B. *Organometallics* **2012**, *30*, 4574.

(15) The standard electrode potential in volts relative to the standard hydrogen electrode at 298.15 K: Te + $2e^-$ = Te^{2-}: −1.143 V; Se + $2e^-$ = Se^{2-}: −0.924 V; S + $2e^-$ = S^{2-}: −0.476 V. (a) Bard, A. J.; Parsons, R.; Jordan, J. *Standard Potentials in Aqueous Solutions*; Marcel Dekker: New York, 1985; (b) Weast, R. C. *Handbook of Chemistry and Physics*, 69th ed.; CRC Press: Boca Raton, FL, 1988−1989; p D-151.

(16) (a) Basuli, F.; Tomaszewski, J.; Huffman, J. C.; Mindiola, D. J. *Organometallics* **2003**, *22*, 4705. (b) Knight, L. K.; Piers, W. E.; Fleurat-Lessard, P.; Parvez, M.; McDonald, R. *Organometallics* **2004**, *23*, 2087. (c) Scott, J.; Basuli, F.; Fout, A. R.; Huffman, J. C.; Mindiola, D. J. *Angew. Chem., Int. Ed.* **2008**, *47*, 8502. (d) Scott, J.; Fan, H. J.; Wicker, B. F.; Fout, A. R.; Baik, M. H.; Mindiola, D. J. *J. Am. Chem. Soc.* **2008**, *130*, 14438. (e) Lu, E. L.; Chu, J. X.; Borzov, M. V.; Chen, Y. F.; Li, G. Y. *Chem. Commun.* **2011**, *47*, 743. (f) Chu, J. X.; Lu, E. L.; Liu, Z. X.; Chen, Y. F.; Leng, X. B.; Song, H. B. *Angew. Chem., Int. Ed.* **2011**, *50*, 7677.

(17) (a) Douglass, M. R.; Stern, C. L.; Marks, T. J. *J. Am. Chem. Soc.* **2001**, *123*, 10221. (b) Krieck, S.; Görls, H.; Westerhausen, M. *Inorg. Chem. Commun.* **2009**, *12*, 409.

(18) (a) Emslie, D. J. H.; Piers, W. E.; Parvez, M.; McDonald, R. *Organometallics* **2002**, *21*, 4226. (b) Yang, Y.; Liu, B.; Lv, K.; Gao, W.; Cui, D.; Chen, X.; Jing, X. *Organometallics* **2007**, *26*, 4575. (c) Meyer, N.; Roesky, P. W.; Bambirra, S.; Meetsma, A.; Hessen, B.; Saliu, K.; Takats, J. *Organometallics* **2008**, *27*, 1501. (d) Zimmermann, M.; Törnroos, K. W.; Waymouth, R. M.; Anwander, R. *Organometallics* **2008**, *27*, 4310. (e) Sadow, A. D.; Tilley, T. D. *J. Am. Chem. Soc.* **2003**, *125*, 7971. (f) Xu, X.; Chen, Y. F.; Sun, J. *Chem.—Eur. J.* **2009**, *15*, 846. (g) Elvidge, B. R.; Arndt, S.; Zeimentz, P. M.; Spaniol, T. P.; Okuda, J. *Inorg. Chem.* **2005**, *44*, 6777. (h) Skinner, M. E. G.; Mountford, P. J. *J. Chem. Soc., Dalton Trans.* **2002**, 1694. (i) Thompson, M. E.; Baxter, S. M.; Bulls, A. R.; Burger, B. J.; Nolan, M. C.; Santasiero, B. D.; Schaefer, W. P.; Bercaw, J. E. *J. Am. Chem. Soc.* **1987**, *109*, 203.

(19) All the structurally characterized complexes are labeled **Xm**, where **m** stands for model.

(20) (a) Charrier, C.; Guilhem, J.; Mathey, F. *J. Org. Chem.* **1981**, *46*, 3. (b) Charrier, C.; Maigrot, N.; Mathey, F.; Robert, F.; Jeannin, Y. *Organometallics* **1986**, *5*, 623. (c) Phillips, I. G.; Ball, R. G.; Cavell, R. G. *Inorg. Chem.* **1988**, *27*, 2269. (d) Ito, S.; Jin, H.; Kimura, S.; Yoshifuji, M. *J. Org. Chem.* **2005**, *70*, 3537.

(21) (a) Evans, W. J.; Wayda, A. L.; Hunter, W. E.; Atwood, J. L. *J. Chem. Soc.,Chem. Commun.* **1981**, 706. (b) Evans, W. J.; Hughes, L. A.; Drummond, D. K.; Zhang, H. M.; Atwood, J. L. *J. Am. Chem. Soc.* **1986**, *108*, 1722. (c) Evans, W. J.; Forrestal, K. J.; Ziller, J. W. *J. Am. Chem. Soc.* **1995**, *117*, 12635.